

Original Article

# Tectonic Setting and Provenance of Metasedimentary Rocks of Taneka Mountain Pan-African Dahomeyide Orogenic Belt, Northwestern Benin Republic

Abdou Wahidou Seidou<sup>1,3\*</sup>, Akinade Shadrach Olatunji<sup>2</sup>, Luc Adissin Glodji<sup>3</sup>, Kouame Saint Blanc Kouassi<sup>1</sup>

<sup>1</sup>Mineral Exploration Program, Pan African University Life and Earth Sciences Institute, University of Ibadan (PAULESI), Oyo State, Nigeria.

<sup>2</sup>Geology Department, University of Ibadan, Oyo State, Nigeria.

<sup>3</sup>Earth Science Department, University of Abomey Calavi, Abomey-Calavi, Benin Republic.

\*Corresponding Author : [alimiyaoseidou@gmail.com](mailto:alimiyaoseidou@gmail.com)

Received: 23 February 2025

Revised: 27 March 2025

Accepted: 13 April 2025

Published: 29 April 2025

**Abstract** - The Taneka Mountain in northwestern Benin Republic lies east of the external and suture zones of the Pan-African Dahomeyide orogenic belt, surrounded by migmatites and gneisses in the crystalline basement. It consists of metasedimentary rocks, mainly quartzites and schists, offering insights into their petrogenesis and tectonic setting. This research focuses on these rocks' petrographic and geochemical features to understand their composition, petrogenesis, provenance, and tectonic context. Twenty samples were collected for thin-section and geochemical analysis. Major oxides, trace elements, and rare earth elements were analyzed using Inductively Coupled Plasma Mass Spectrometry (ICP-MS) at Activation Laboratory Ltd, Canada. Petrography reveals that quartzites are dominated by quartz and muscovite, with minor amounts of tourmaline, while schists contain talc, quartz, and chlorite. A geochemical study suggests that quartzites are siliceous (SiO<sub>2</sub>: 82.18 wt.%) with low other oxides, suggesting mature sedimentary origins. Schists have higher Al<sub>2</sub>O<sub>3</sub> (14.68 wt.%) and Fe<sub>2</sub>O<sub>3</sub> (5.13 wt.%), indicating pelitic protoliths. Trace and REE data distinguish the lithologies: quartzites show depleted trace elements, whereas schists are enriched. The geochemical findings indicate that the quartzites originated from mature, quartz-rich sediments, possibly derived from felsic terrains. At the same time, the schists have a heterogeneous sedimentary provenance with contributions from both felsic and mafic rocks. The tectonic context of the quartzites is consistent with a passive margin, whereas the schists indicate a transitional environment influenced by surrounding active tectonic zones. The tectonic setting and provenance of the Taneka Mountain quartzites and schists are similar to those of the external zone of the Pan-African orogeny.

**Keywords** - Benin, metasedimentary rocks, passive margin, Pan-African orogeny, Taneka Mountain transitional environment.

## 1. Introduction

The Taneka Mountain, located in the commune of Copargo in the northwestern Benin Republic (Figure 1), is an area of geological importance within the Pan-African Dahomeyide orogenic belt. This region is characterized by its complex tectonic history and metasedimentary rocks, including quartzites and schists, which are analogous to those found in the external zone of the Dahomeyide belt. The Dahomeyide belt formed during the late Neoproterozoic to early Cambrian due to convergence between the West African Craton (WAC) and other continental margins. [1,2,3,4,5] The belt is divided into three structural units: the external zone, internal zone, and suture zone, each exhibiting distinct geological features and rock types. [6,7,8]. Despite extensive studies on the Dahomeyide belt, significant gaps remain in understanding the geological and mineralogical attributes of the metasedimentary rocks in the Taneka Mountain area.

Previous research has focused primarily on the Atacora Structural Unit (ASU) within the external zone, where gold-bearing metasedimentary rocks have been well-documented [9].

However, Taneka Mountain, which lies within the internal zone of the belt (Figure 2), has received limited attention, and petrogenesis, tectonic setting, and provenance are poorly understood. This lack of knowledge obstructs a thorough grasp of the regional geological evolution and extensive tectonic processes related to the Pan-African orogeny in West Africa. The lack of detailed studies on Taneka Mountain metasedimentary rocks presents a critical problem: without a precise characterization of their petrographic and geochemical signatures, correlating their formation history with the well-studied ASU becomes challenging, as does reconstructing the paleoenvironmental and tectonic conditions that shaped this



part of the Dahomeyide belt. This study aims to bridge this gap by systematically investigating the petrographic and geochemical characteristics of the quartzites and schists in the Taneka Terrane. By analyzing their mineral compositions, geochemical signatures, and structural features, we seek to determine the provenances and tectonic settings of these rocks, assess their metamorphic history and conditions, and

compare their attributes with those of the ASU to evaluate their role in the evolution of the Dahomeyide belt.

The findings enhance our understanding of the Taneka Terrane and contribute to the broader framework of the Pan-African orogeny in West Africa, providing insights into the geodynamic processes that shaped this region. [10, 11]

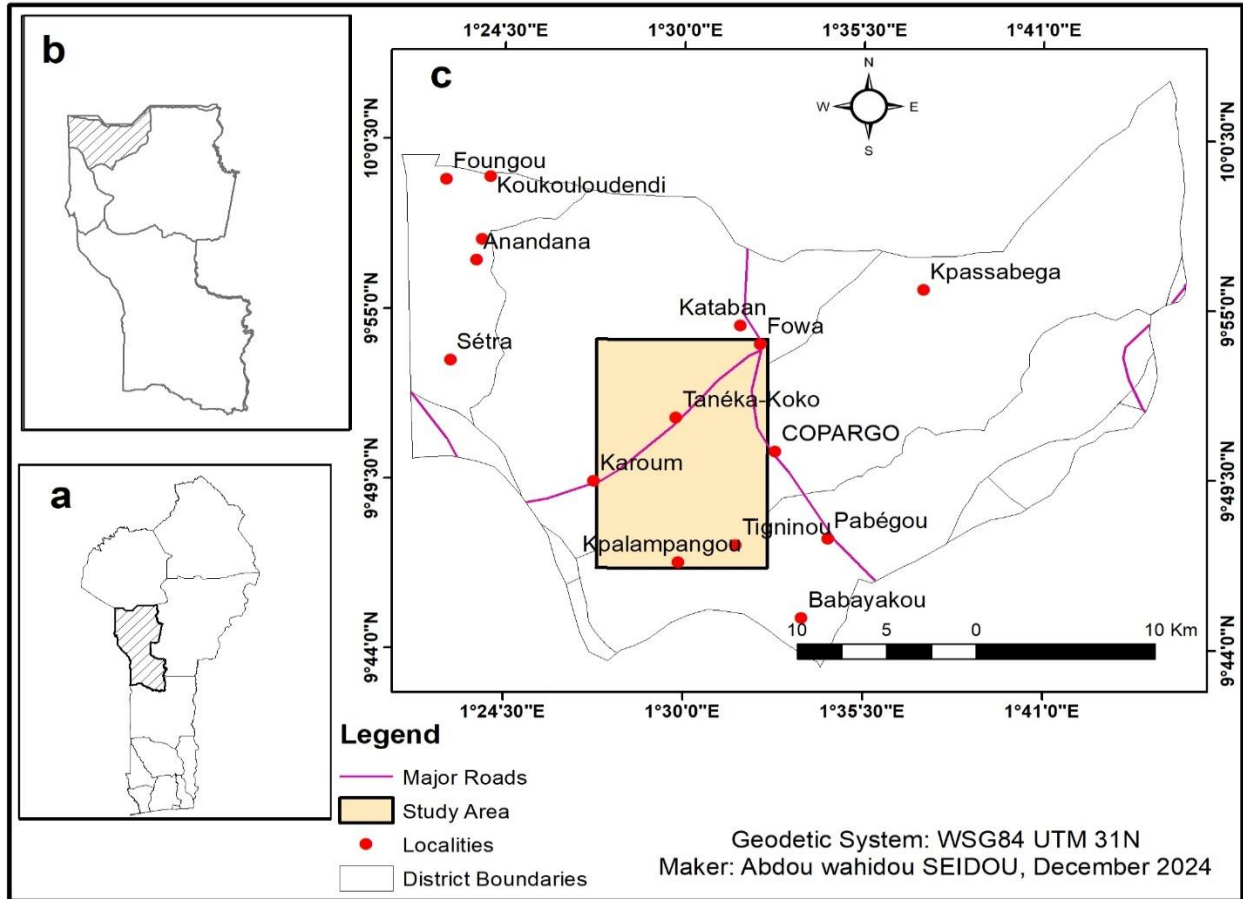


Fig. 1 Location of the Study Area, (a)Map of Benin Republic showing the Donga Department, (b)Department of Donga with the commune of Copargo, (c)Study area in the commune of Copargo

## 2. Regional Geological Setting

The West African Craton (WAC) is one of the oldest and most stable geological regions in West Africa and is composed primarily of Archean and Paleoproterozoic rocks. The area is rich in mineral resources and has several first-grade gold deposits. The craton consists of high-grade gneisses, magmatic formations, and greenstone belts formed by ancient geodynamic processes that have been traced back more than 2.5 billion years. [2, 12] Around the WAC, young mobile belts, such as the Pan-African Dahomeyide Orogen, have heavily influenced the geological evolution of the area. [11, 13, 14]. The Dahomeyide Orogenic Belt emerged during the Pan-African orogeny, a tectonic event that unfolded from approximately 600 to 500 million years ago, spanning the late Neoproterozoic to early Cambrian periods. This orogeny was triggered by the eastward subduction of Neoproterozoic

passive margin sediments and Pharusian oceanic crust beneath the West African Craton, ultimately leading to a continental collision between the WAC and the Benino-Nigerian Shield (BNS). [5, 6, 15-20] Structurally, the Dahomeyide Belt is subdivided into three central tectonic units, the external zone, suture zone, and internal zone, each displaying distinct lithological and metamorphic characteristics [1, 6, 7, 10, 20]. The External Zone features thrust nappes formed from sedimentary sequences that underwent medium- to high-pressure metamorphism. It includes two main structural subdivisions: The Buem Structural Unit (BSU), which consists of massive arkoses and a thick accumulation of fine-grained sediments (shales, siltstones, mudstones), along with chert, limestone, and interstratified mafic to felsic volcanic rocks. Within this unit, ultramafic rocks are often serpentinized. [5, 7, 18, 21-30] The Atacora Structural Unit

(ASU), which consists of quartzite, quartzitic sandstone, schists, and phyllites, has undergone upper greenschist to lower amphibolite facies metamorphism [2,5,6,7]. The Suture Zone signifies the collisional boundary between the WAC and the BNS.

This area is characterized by a mélange of deformed rocks, incorporating high-to ultrahigh-pressure (HP-UHP) rocks, high-pressure granulites, amphibolites, pyroxenites, and various alkaline to calc-alkaline intrusions, including carbonatites. [5, 19, 20, 28, 29, 31-35] Basic and ultrabasic massifs, metasedimentary sequences, and orthogneisses are tectonically located between the External and Internal zones [2,7,10,36]. The Internal Zone comprises high-grade metamorphic rocks intruded by granitoid plutons and associated with volcano-sedimentary basins.

It includes Archaean-derived migmatitic and anatectic rocks such as granite, charnockite, orthogneiss, and granulite, alongside metasedimentary units such as marbles, quartzites,

and mica schists. [37-43] It is structurally intricate, with notable tectonic overprints, including shear zones such as the Kandi Shear Zone [18].

**2.1. Geology of Benin**

In the context of Benin, the Dahomeyide orogenic belt plays a substantial role in the nation's geology. The Beninese segment of the belt consists of a crystalline basement topped by sedimentary layers, categorized into six central regions: the coastal sedimentary basin, the Kandi sedimentary basin; the external, suture, and internal zones of the Dahomeyide belt, and the Volta sedimentary basin. The crystalline basement in Benin, which is part of the internal zone of the Pan-African Dahomeyide Belt, is characterized by high-grade metamorphic complexes and plays a crucial role in understanding the tectonic and sedimentary history of the area. [6]. The study area, located in the internal zone of the Dahomeyide Belt, presents an optimal environment for exploring the provenance and tectonometamorphic evolution of metasedimentary rocks in a Pan-African collisional context.

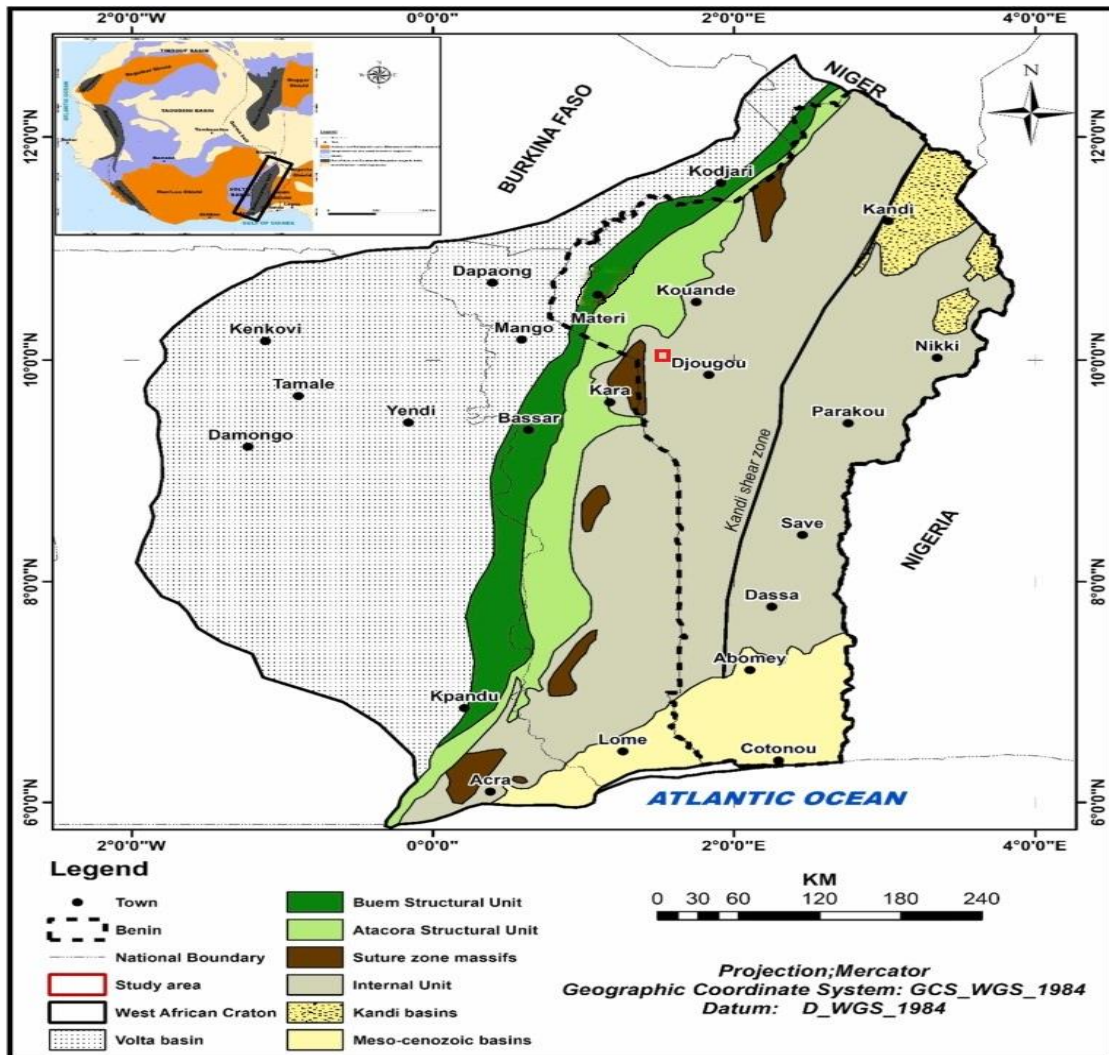


Fig. 2 Illustrating the primary components of the Pan-African Dahomeyides belt and the study area [24]

### 3. Materials and Methods

Comprehensive geological mapping of the Taneka area was conducted, and new rock samples were collected for petrographic and geochemical analysis. Fifteen (15) samples of fresh and representative rock among the 20 samples were brought to the Department of Geology at Obafemi Awolowo University in Ile-Ife, Nigeria, for thin section preparation and studies. The standard technique of thin-section preparation was used to carefully cut the rock samples into thin slices, which were then mounted on glass slides with epoxy. After 24h, the thin slices were ground down to a thickness of 30 micrometres via a precision grinder and covered with a protective slip to increase their clarity under the microscope.

The prepared sections were then examined under a petrographic microscope at the Department of Geology of the University of Ibadan in Nigeria. Detailed petrographic studies were conducted on the mineral composition, texture, grain size, grain shape, structure, and modal percentage of minerals in the rocks to confirm their names. Ten (10) samples (7 quartzites and 3 schists) were selected for geochemical analysis and sent to Activation Laboratories Ltd. in Ancaster, Ontario, Canada. The samples were crushed and pulverized before they were subjected to whole rock analysis, including

rare earth elements and major and trace elements via inductively coupled plasma mass spectrometry and Optical Emission Spectroscopy (ICP-MS + ICPOES). The samples were mixed with sodium peroxide. Georse, Gcdkit Graphpad, and Surfer were the software used to generate structural and geochemical diagrams during this work.

### 4. Results

#### 4.1. Field Description and Structures

Detailed analysis of the structural elements observed in the Taneka Terrane, focusing on geological field observations and measurements of ductile and brittle structures. The key structural features include foliations/schistosity, joints, folds, and fractures. Recumbent folds are observed in quartzite outcrops (Figure 3a), and asymmetric folds are present in schist outcrops (Figure 3b). Foliations predominantly trend NE-SW with varying dip values (Figure 4a). At the same time, joints (nonsystematic cross-cutting joint pattern, Figure 3c, and parallel joints, Figure 3d) are the most abundant brittle structures, also trending mainly in the NE-SW and NW-SE directions. Fractures are primarily oriented NE-SW and NW-SE (Figure 4a), often associated with quartz veins. The comprehensive structural analysis reveals a poly deformational history aligned with the Pan-African orogeny.

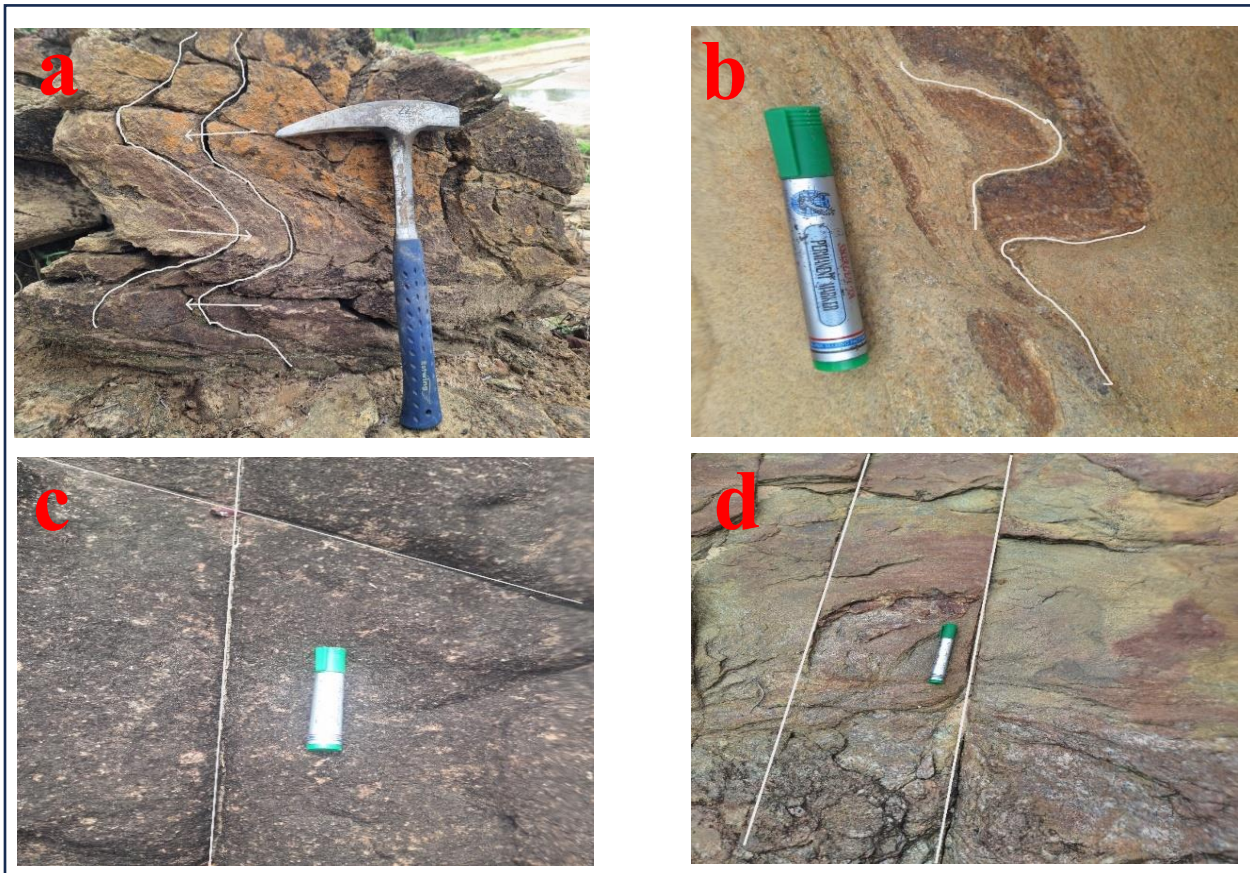


Fig. 3 (a)Field photograph showing recumbent fold in quartzite outcrop, (b)Field photograph showing asymmetric fold in schist outcrop, (c)Field photograph of a nonsystematic cross-cutting joint pattern in quartzite outcrops, and (d)Field photograph showing parallel joints pattern in schist outcrop

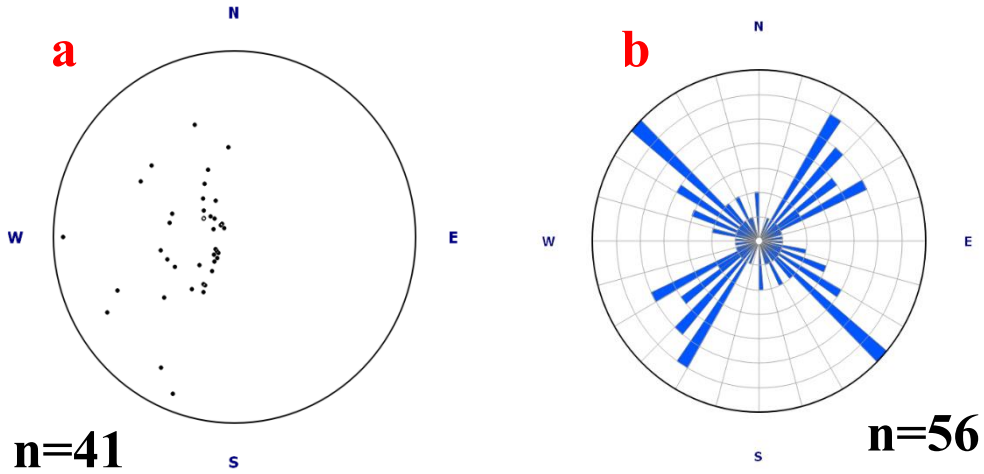


Fig. 4 (a)Plot (full circle) of poles of foliations planes of rocks, (b)Rose diagram plot of fractures in the field throughout the study area shows the following directions: NE-SW and NW-SE

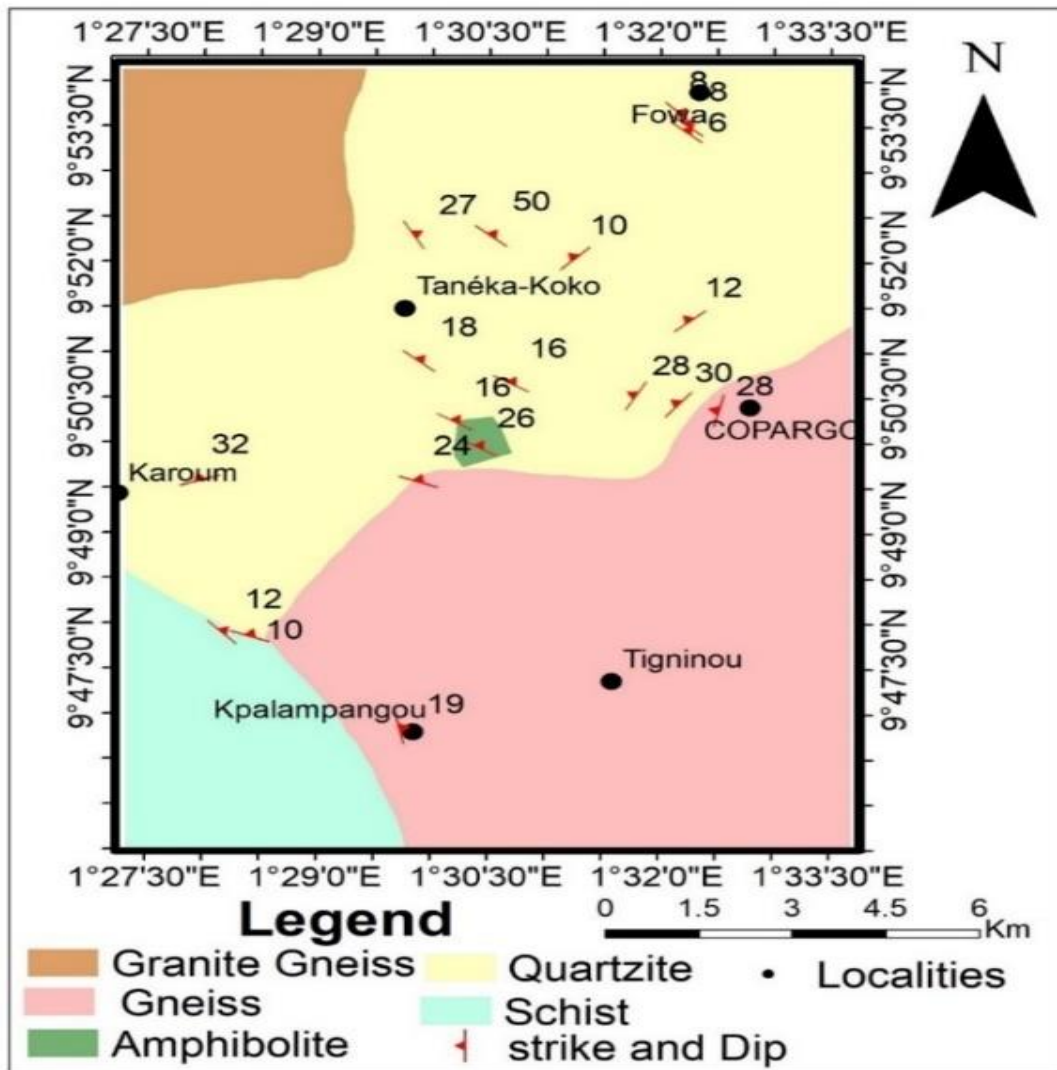


Fig. 5 Geological map of the study area (Modified after DJOUGOU-PARAKOU-NIKKI Geological sheet)

**4.2. Petrography**

**4.2.1. Quartzites**

They constitute a monotonous appearance in the study area. These are light-colored rocks that are generally whitish, very compact, and often cut into large slabs due to the deformation effect. Three types of quartzite can be distinguished in the study area: the very common type has a fine grain size, such as those from the Tanéka-Koko and Tanéka-Béri localities; the second type is more saccharoidal with medium quartz grains, such as those from the Yaka locality and the third type (Quartz muscovite schist) has exudation quartz (metamorphic quartz). We found them above the mica schist. The Hand specimens are generally whitish-grey, fine to medium-grained in texture, and are composed of quartz and white mica (Figure 7a). They are the same rock with variations in the amount of muscovite present. Under the microscope, they exhibit a granolepidoblastic structure composed of quartz grains and muscovite of all types (Figure 8b). In the first and second types, muscovite appears in long streaks of fine-oriented flakes, whereas in the third type, it appears in thicker flakes with no very visible orientation. It has more muscovite content than the previous sample. The accessory mineral is tourmaline. The modal composition of the quartzite is shown in Table 1.

**4.2.2. Mica Schists/Schists**

Mica schists are found among quartzites in layers of highly variable thickness, ranging from a few centimetres to several decimetres. They are encountered more often in the southwest of the studied area. Notably, they become increasingly rare and are often completely absent from the centre to the far north of the studied region. They are mainly found west of the Tomi locality, particularly in the Sensitru River, where they are readily observable and associated with quartz veins in the good vertical cuts visible in the gorges carved by this river.

At the outcrop scale, mica schists are less frequently observable due to their high susceptibility to weathering. The lenticular chlorite schist is usually present in the micaschist. The schist outcrops were also folded. The mica schist has a lepidoblastic texture and is medium to coarse-grained (Figure 7b). The chlorite-schist exhibits greyish to greyish-brown weathering colourations in place. The mica schist sample selected for the thin section was associated with a quartz vein, and the section cut the quartz part and contained only quartz. In a thin section (Figure 8b), the schist contains the platy minerals talc, quartz and chlorite. The modal composition is shown in Table 1 and Figure 6.

**Table 1. Modal composition of metasedimentary rocks in the Taneka area**

Minerals	Quartzites			Quartz Muscovite Schist	Schist
	COR10	COR02	COR19	COR14	COR15
<b>Quartz</b>	85	94	70	70	30
<b>Muscovite</b>	15	6	25	30	-
<b>Tourmaline</b>	-	-	5	-	-
<b>Talc</b>	-	-	-	-	60
<b>Chlorite</b>	-	-	-	-	10

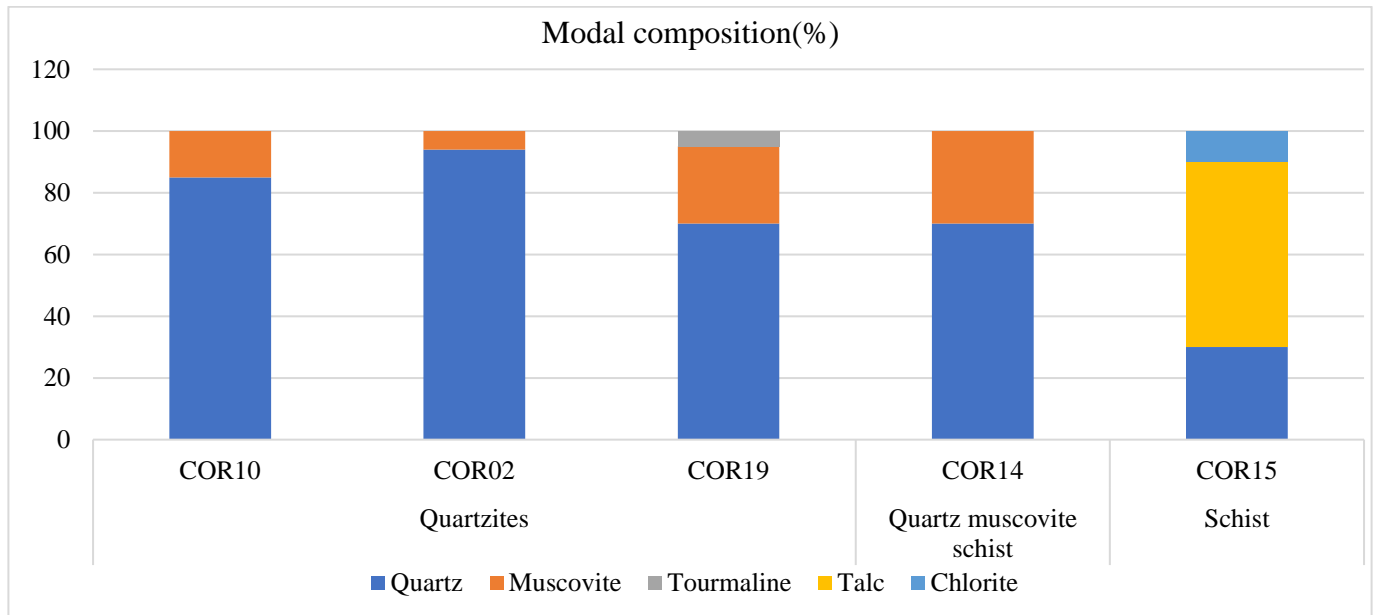


**Fig. 6 Graphic showing the modal composition of the rocks**



Fig. 7(a) Hand specimen of Quartzite from Taneka Koko region showing fine grain size, and (b) Hand specimen of Schist outcrop from the Tomi region (Sensitru river)

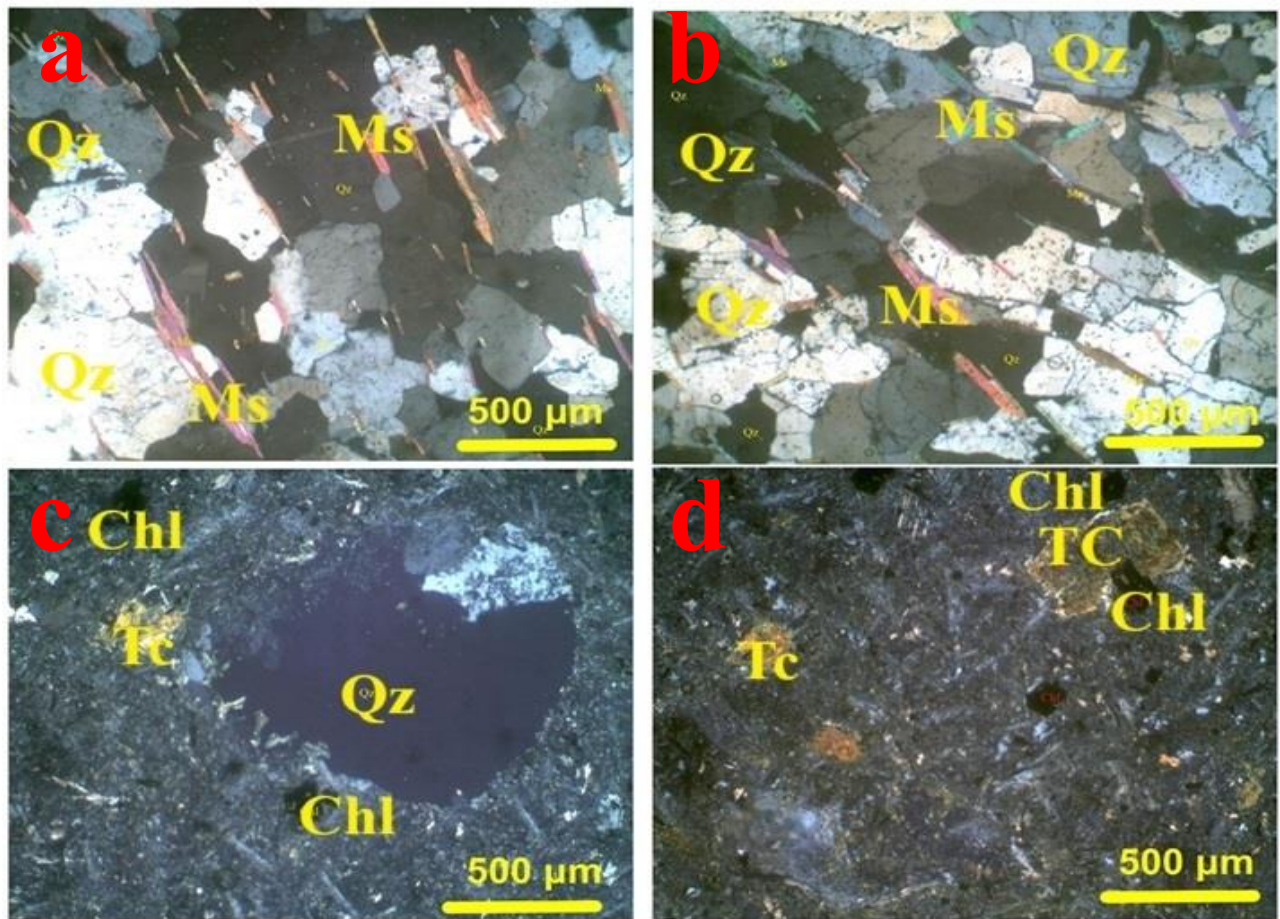


Fig. 8 Photomicrographs of a,b- Quartzite showing Qz-quartz; Ms-muscovite in Cross polarized light view (Xpl); c,d- schist showing Qz-quartz; Chl-Chlorite, Tc- Talc in Cross polarized light view (XPL)

### 4.3. Whole Rock Geochemistry

#### 4.3.1. Major Oxides

The results of the rock compositions of the quartzites and schists in the study area are presented in Table 2. The quartzites have high siliceous content, with SiO<sub>2</sub> concentrations ranging from 73.59 to 96.91 wt.%, with an average of 82.18 wt.%. In contrast, the schists have SiO<sub>2</sub> concentrations between 68.46 and 74.02 wt.%, averaging 70.03 wt.%. The Al<sub>2</sub>O<sub>3</sub> content in the quartzites varies slightly from 1.49 to 3 wt.% (mean 2.03 wt.%), whereas the schists have a relatively high average Al<sub>2</sub>O<sub>3</sub> concentration of 14.38 wt.% (ranging from 13.22 to 16.34 wt.%). The additional oxides present in the quartzites included Fe<sub>2</sub>O<sub>3</sub> (0.54-0.72 wt.% with mean 0.63), MgO (0.02-0.08 wt.%), K<sub>2</sub>O (0.24-0.96 wt.%), TiO<sub>2</sub> (0.03-0.08 wt.%), and CaO (0.01-0.08 wt.%) (Table 3), whereas in the schists, the concentrations included Fe<sub>2</sub>O<sub>3</sub> (4.63-5.68 wt.% with a mean of 6.64), MgO (1.21-1.46), CaO (0.57-1.54), K<sub>2</sub>O (1.33-1.81), and TiO<sub>2</sub> (0.47-0.68) (Table 2). The connections between Al<sub>2</sub>O<sub>3</sub> and other major oxides demonstrate a strong positive correlation of Al<sub>2</sub>O<sub>3</sub> with TiO<sub>2</sub>, Fe<sub>2</sub>O<sub>3</sub>, MgO, K<sub>2</sub>O, and CaO (Coefficients of correlation R = 0.99, 0.99, 0.97, 0.93 and 0.89, respectively) (Figure 9a), indicating that these rocks are aluminous. SiO<sub>2</sub> strongly negatively correlated with TiO<sub>2</sub>, Fe<sub>2</sub>O<sub>3</sub>, and Al<sub>2</sub>O<sub>3</sub> but moderately or weakly correlated with MgO, CaO, and K<sub>2</sub>O (Figure 9b). These findings indicate that these rocks originated from a recycled sedimentary source or the removal of ferromagnesian and feldspar minerals. [44]

#### 4.3.2. Trace Elements

The trace element compositions of Taneka metasedimentary rocks are presented in Table 2. The trace element compositions reveal distinct profiles for quartzites and schists (Table 2). Quartzites contain LILE elements such as Ba (23-228 ppm, average of 94.29), Rb (7.80-32.70 ppm, average of 17.43), and Cs (0.70-3.20 ppm, average of 1.66). The concentrations of other trace elements in the quartzites included Ni (20-30 ppm), Cu (4-18 ppm), Zn (30-50 ppm), Pb (6.90-61.60 ppm), and W, Mo, and Sn in lower ranges (Table 2). For schists, Ba (390-496 ppm, average of 440.33), Sr (240-256 ppm, average 250), Cr (110-130 ppm, average of 116.67), and Zn (70-90 ppm, average 80) are significantly enriched. Slight enrichments in Ni (50-70 ppm, average of 60), Rb (52.60-68.20 ppm, average of 58.47), and other trace elements such as Cu (26-47 ppm, average of 35), Li (35-39 ppm, average of 36.67), and Co (16.5-20.3 ppm, average of 18.83) are also observed (Table 2).

#### 4.3.3. Rare Earth Elements

The rare earth element compositions for both quartzites and schists in the study area are presented in Table 2. In terms of rare earth elements (REE), quartzites demonstrate variations with enrichments in LREE as shown in the chondrite-normalized REE patterns (Figure 10a), characterized by LaN/SmN ratios (2.85-6.67) and negative Eu anomalies (0.10-0.27). The schists, normalized via Boyton,

show similar trends, with a strong LREE enrichment, a flat HREE profile, and slight negative Eu anomalies (Figure 10a). The (Eu/Eu\*)<sub>N</sub> values range from 0.27-0.34 for schists, with La/Sm ratios ranging from 4.19-5.07 and total REE concentrations ranging from 152.3 to 195.7 ppm (Table 2).

## 5. Discussion

### 5.1. Metamorphism Conditions of the Rocks in the Taneka Area

The metasedimentary rocks of Taneka Mountain exhibit mineral assemblages indicative of greenschist facies metamorphism, as evidenced by the quartz-muscovite association in quartzites and talc-chlorite-quartz assemblage in schists. According to [46], these mineral parageneses suggest metamorphic conditions of 300-450°C and 4-8 kbar for quartzites and slightly lower temperatures (250-400°C) for schists, as described by [45]. Muscovite without higher-grade aluminosilicates implies that the rocks experienced regional metamorphism without reaching upper greenschist or amphibolite facies conditions. Structurally, the area displays recumbent folding consistent with compressional deformation during nappe emplacement in the Pan-African orogeny, followed by the development of NE-SW trending fractures that may represent late-stage brittle deformation. The metamorphic grade and structural style suggest that Taneka Mountain occupied a more distal position in the orogenic system than did to the higher-grade Atacora Structural Unit, with deformation occurring under moderate pressure-temperature conditions, followed by limited post-collisional exhumation that preserved the greenschist facies mineralogy. [45,46] These features collectively indicate that the rocks underwent burial metamorphism and compressional deformation during continental collision but were not subjected to intense thrusting or higher-grade metamorphic characteristics of more internal zones in the Dahomeyide Belt.

### 5.2. Petrogenesis, Tectonic Setting and Provenance of Metasedimentary Rocks in Taneka Mountain

The metasedimentary rocks (quartzite and schist) of the Taneka area exhibit distinct compositional and provenance characteristics, reflecting their unique origins and tectonic settings. Quartzites are characterized by exceptionally high SiO<sub>2</sub> contents (82.18 wt.%) with minimal contributions from other oxides (Al<sub>2</sub>O<sub>3</sub>: 2.03 wt.%, Fe<sub>2</sub>O<sub>3</sub>: 0.63 wt.%), indicating their derivation from mature, quartz-rich sediments. [47,48] In contrast, schists exhibit a more diverse mineralogical composition with moderate SiO<sub>2</sub> (71.88 wt.%), elevated Al<sub>2</sub>O<sub>3</sub> (14.68 wt.%), and significant Fe<sub>2</sub>O<sub>3</sub> (5.13 wt.%), reflecting their pelitic precursor and subsequent metamorphic recrystallization. [49,50]. Trace element patterns further differentiate these lithologies. Quartzites show depleted trace element concentrations (Ba: 94.29 ppm, Cu: 8.57 ppm), consistent with their mature sedimentary origin and limited chemical alteration. [51,52] Schists display enriched trace element signatures (Ba: 440.33 ppm, Cu: 35.00 ppm), suggesting a more diverse source composition and possible

hydrothermal modification during metamorphism. [53] REE distributions provide crucial insights into the petrogenetic history of these rocks. Quartzites exhibit relatively low total REE contents ( $\Sigma$ REE: 31.83 ppm) with pronounced LREE/HREE fractionation ( $(\text{La}/\text{Yb})_{\text{CN}} = 13.13$ ) and relatively flat REE patterns, indicating minimal metamorphic modification. [54] In contrast, schists show significantly higher  $\Sigma$ REE (167.43 ppm) with marked LREE enrichment (132.27 ppm) than HREE (35.17 ppm) and more complex REE patterns with pronounced LREE peaks, reflecting their polyphase metamorphic evolution. [51, 55]. The figure plotting  $\text{K}_2\text{O}$  (W%) against  $\text{Na}_2\text{O}$  (W%) is used to classify the Taneka metasedimentary rocks into quartz-rich, quartz-intermediate, and quartz-poor. Based on the geochemical data, both the quartzite and schist samples exhibit very low  $\text{K}_2\text{O}$  (0.01 W%) and low  $\text{Na}_2\text{O}$  (0.1 W%) values, placing them in the quartz-rich category (Figure 10b). This indicates that the protoliths were highly mature sedimentary rocks, likely derived from well-weathered and sorted quartz sandstones. The low alkali content reflects minimal contributions from feldspar or lithic fragments. [48, 56]

The geochemical discrimination diagrams show that quartzite and schist have distinct provenance characteristics. On the  $\log(\text{SiO}_2/\text{Al}_2\text{O}_3)$  vs.  $\log(\text{Fe}_2\text{O}_3/\text{K}_2\text{O})$  diagram after [47], quartzite plots predominantly in the “Quartz arenite” and “Sublitharenite” fields (Figure 11.a), reflecting its high silica content and low  $\text{Fe}_2\text{O}_3$  and  $\text{K}_2\text{O}$  values. This suggests derivation from mature, quartz-rich sediments formed through extensive weathering and sedimentary recycling, likely sourced from felsic (granitic) terrains. [54] On the other hand, Schist plots in the “Shale” and “Wacke” fields, with relatively high  $\text{Fe}_2\text{O}_3$  and  $\text{Al}_2\text{O}_3$  contents, indicating clay-rich protoliths with moderate maturity. This composition suggests a mixed sedimentary source, including felsic and mafic rocks [57].

The discrimination diagram ( $\text{Zr}$  vs.  $\text{TiO}_2$ ) further supports these interpretations (Figure 11.c). Quartzite plots near the origin, with very low  $\text{Zr}$  and  $\text{TiO}_2$  concentrations, consistent with a highly mature source dominated by silica-rich sediments derived from felsic rocks such as granite or rhyolite. Schist plots at slightly higher  $\text{TiO}_2$  ( $\sim 0.5$ ) and  $\text{Zr}$  ( $< 50$  ppm) values, indicating derivation from a mixture of felsic to intermediate sources. These compositions suggest minimal contributions from mafic rocks. [54]

The discrimination diagram ( $\text{K}_2\text{O}/\text{Na}_2\text{O}$  vs.  $\text{SiO}_2$ ) after [48] reveals the tectonic settings of the rocks (Figure 11d). Quartzite plots distinctly within the Passive Margin (PM) field, characterized by high silica content ( $\sim 90\%$   $\text{SiO}_2$ ) and elevated  $\text{K}_2\text{O}/\text{Na}_2\text{O}$  ratios ( $> 10$ ), indicative of a stable tectonic environment with quartz-rich sediments deposited in passive continental margins. While predominantly within the Passive Margin (PM) field, Schist lies closer to the boundary with the Active Continental Margin (ACM) field. With slightly lower silica content ( $\sim 70\%$   $\text{SiO}_2$ ) and intermediate

$\text{K}_2\text{O}/\text{Na}_2\text{O}$  ratios ( $\sim 5$ – $10$ ), the schist reflects a transitional environment influenced by sediments from nearby active tectonic regions. [58] In the  $\text{La}/\text{Yb}$  vs.  $\Sigma$ REE provenance discrimination diagram, quartzite falls within the “Sedimentary rocks” field (Figure 11b). Its high  $\text{La}/\text{Yb}$  ratios and moderate  $\Sigma$ REE values confirm its origin from continental crust materials, specifically granitic terrains. Schist also falls within the category of sedimentary rocks. Nevertheless, it has higher  $\Sigma$ REE values and lower  $\text{La}/\text{Yb}$  ratios, reflecting a less mature sedimentary protolith influenced by felsic and mafic contributions. [56]

### 5.3. Comparison with the ASU of the External Zone of the Pan-African Dahomeyide belt

The metasedimentary rocks of Taneka Mountain and the Atacora Structural Unit (ASU) share lithological similarities but differ in metamorphic grade and structural evolution, reflecting their distinct positions within the Dahomeyide Belt. Both units consist primarily of quartzites and schists, with Taneka’s quartzites (average 82.18 wt.%  $\text{SiO}_2$ ) being slightly less siliceous than those of the ASU (88–94 wt.%  $\text{SiO}_2$ ). [9] The schists in both regions originate from pelitic protoliths; however, Taneka’s schists are characterized by quartz-talc-chlorite assemblages, indicating lower greenschist-facies conditions. In contrast, the ASU schists contain biotite, garnet, and epidote, suggesting upper greenschist to lower amphibolite-facies metamorphism. [9, 33]. Provenance analysis reveals that both units were sourced from felsic (granitic/gneissic) terrains, supported by their high  $\text{SiO}_2$  content and negative Eu anomalies, consistent with passive margin sedimentation. [48] However, the ASU schists exhibit stronger arc-related signatures, likely due to their proximity to the Dahomeyide suture zone, whereas Taneka’s metasedimentary rocks reflect a more stable continental margin setting. Structurally, the ASU underwent intense thrust-dominated deformation, with NE-SW shear zones controlling gold mineralization. In contrast, Taneka exhibits recumbent folding and brittle fracturing, suggesting a more distal position within the orogen. [1, 9]

The contrast in metamorphic facies is significant: Taneka rocks record greenschist-facies conditions, characterized by chlorite-muscovite assemblages, whereas the ASU exhibits amphibolite-facies characteristics (garnet-biotite-epidote), indicating deeper burial and/or greater tectonic stresses during the Pan-African orogeny ( $\sim 600$ – $500$  Ma). [1, 9] This difference is consistent with the ASU’s role as part of the externally thrust nappes, whereas Taneka may represent a hinterland or back-thrust domain with less intense metamorphism. Further geochronological and isotopic studies could clarify their precise tectonic relationship; however, current evidence suggests that both units are complementary components of the Dahomeyide Belt, with the ASU denoting the high-strain, mineralized thrust front and Taneka preserving a less deformed, lower-grade section of the same metasedimentary system.

**5.4. Comparison with Other Metasedimentary Rock Studies**

Compared with similar rocks from other orogenic belts worldwide, the metasedimentary rocks of Taneka Mountain in the northwestern Benin Republic exhibit distinct characteristics. [59] studied the South Delhi Supergroup in NW India, where metasedimentary rocks show strong arc-related signatures with high Th/Sc and Zr/Sc ratios, indicating significant crustal recycling, in contrast to Taneka's passive margin quartzites, which have lower trace element enrichment. However, similar to Taneka, their schists display mixed felsic-mafic provenances, suggesting transitional tectonic settings in both regions. According to [59], the metasedimentary rocks are deposited in the South Delhi Supergroup in the passive margin similar to those in Taneka. In West Africa, [56] studied metasediments from Nigeria's Kabba-Lokoja-Igarra schist belt and reported higher-grade amphibolite-facies assemblages (garnet-staurolite schists) than did Taneka's greenschist-facies talc-chlorite schists. Both regions, however, share similar passive margin affinities in quartzites, reinforcing the prevalence of stable cratonic sedimentation before Pan-African deformation. Similarly, [52] reported quartz-mica schists in SW Nigeria with comparable SiO<sub>2</sub> enrichment (68.04-80 wt.%) to that of the Taneka quartzites, although Nigerian samples present stronger

Eu anomalies, indicating more felsic source rocks [56, 52]. [54] examined graywackes and siltstones in Mali's Nampala gold deposit. According to Konate, these rocks comprise immature to moderate sediment, whereas Taneka's rocks are mature sediment. Unlike Taneka's mature quartzites, these rocks have an active continental margin source. This aligns with findings from [61] in Ghana's Birimian belt, where metasediments share similar active continental margin affinities and show higher Cr and Ni contents, reflecting stronger mafic input than that observed in Taneka. Further comparisons with [62] in Ghana's Kumasi Basin reveal that, like Taneka, their rocks underwent moderate weathering but differed in having more pronounced negative Eu anomalies, suggesting longer sediment recycling. Finally, [63] studied the Singhbhum Craton in India, where metasedimentary rocks record Archean provenances (3.2 Ga detrital zircons), unlike Taneka's Neoproterozoic Pan-African signatures. Taneka's quartzites resemble passive margin deposits (similar to those in Nigeria and India) but lack the high-grade metamorphism observed in Mali and Ghana. The schist compositions vary widely: Taneka's talc-chlorite assemblages indicate lower-grade conditions than Nigerian garnet-staurolite schists. The provenance signatures in Taneka suggest less mafic input than those in Mali's Nampala or Ghana's Birimian rocks.

**Table 2. Major, Trace and Rare earth elements compositions of metasedimentary rocks of Taneka**

Rocks type	Quartzite							Average	Schists			
	COR07a	COR07b	COR07c	COR19	COR02	COR03	COR14		COR15a	COR15b	COR15c	Average
<b>Major oxides (wt.%)</b>												
Al <sub>2</sub> O <sub>3</sub>	1.87	1.7	1.57	1.87	1.49	3	2.72	2.03	13.22	16.34	14.49	14.68
CaO	0.08	0.06	0.07	0.08	0.06	0.01	0.07	0.06	0.57	1.54	0.6	0.9
Fe <sub>2</sub> O <sub>3</sub>	0.54	0.61	0.54	0.72	0.69	0.67	0.63	0.63	4.63	5.68	5.09	5.13
K <sub>2</sub> O	0.6	0.48	0.48	0.6	0.24	0.24	0.96	0.52	1.33	1.81	1.57	1.57
MgO	0.05	0.05	0.05	0.05	0.02	0.05	0.32	0.08	1.46	1.21	1.26	1.31
TiO <sub>2</sub>	0.03	0.03	0.03	0.03	0.05	0.08	0.07	0.05	0.47	0.68	0.5	0.55
SiO <sub>2</sub>	82.15	80.22	75.09	82.79	84.5	73.59	96.91	82.18	74.02	68.46	73.16	71.88
<b>Total</b>	<b>85.33</b>	<b>83.16</b>	<b>77.84</b>	<b>86.15</b>	<b>87.04</b>	<b>77.66</b>	<b>101.68</b>	<b>85.55</b>	<b>95.7</b>	<b>95.72</b>	<b>96.67</b>	<b>96.03</b>
<b>Trace Elements (ppm)</b>												
As	< 5	< 5	< 5	< 5	< 5	< 5	< 5		5	7	10	7.33
Ba	66	61	63	71	23	148	228	94.29	435	496	390	440.33
Co	1.3	0.8	1.3	1	8.9	2.4	2.4	2.59	16.5	19.7	20.3	18.83
Cr	< 30	< 30	< 30	< 30	< 30	< 30	< 30		130	110	110	116.67
Cs	2.3	1.9	1.3	3.2	0.8	0.7	1.4	1.66	1.6	2.5	1.9	2.00
Cu	8	18	4	6	6	12	6	8.57	32	47	26	35.00
Ga	2.1	1.5	1.9	2.2	2.3	3.4	3.4	2.40	12.9	19.5	15.4	15.93
Hf	< 10	< 10	10	< 10	< 10	< 10	< 10	10.00	10	< 10	20	15.00
Li	< 15	< 15	< 15	< 15	< 15	< 15	< 15	0.00	39	35	36	36.67
Mo	3	4	2	2	2	4	1	0.00	3	3	2	2.67

<b>Nb</b>	< 2.4	< 2.4	< 2.4	< 2.4	< 2.4	< 2.4	< 2.4		5.3	9.2	4.4	6.30
<b>Ni</b>	20	20	20	20	20	30	20	21.43	50	70	60	60.00
<b>Pb</b>	11.4	9.6	11	19.9	9.9	6.9	61.6	18.61	11.8	15	11.5	12.77
<b>Rb</b>	18.6	17.2	17	18.2	7.8	10.5	32.7	17.43	52.6	68.2	54.6	58.47
<b>Sn</b>	< 0.5	< 0.5	< 0.5	0.8	0.6	0.5	0.7	0.65	1.6	0.7	1.5	1.27
<b>Sr</b>	19	19	22	22	19	20	18	19.86	256	254	240	250.00
<b>Ta</b>	0.8	1.1	1.3	0.8	1.2	1.5	0.5	1.03	1	1.4	1.1	1.17
<b>Th</b>	1.3	1.1	1.2	1.1	1.7	1.4	1.9	1.39	3.2	5.6	3.2	4.00
<b>U</b>	1.1	0.8	1	1.1	0.6	0.5	0.8	0.84	1.2	2.1	1.5	1.60
<b>W</b>	3.5	< 0.7	< 0.7	0.8	< 0.7	< 0.7	< 0.7	2.15	1.3	1.9	3.2	2.13
<b>Zn</b>	< 30	30	30	< 30	< 30	50	< 30	36.67	80	70	90	80.00

Table 2. (continue)

<b>Rocks type</b>	<b>Quartzite</b>									<b>Schists</b>			
<b>Sample code</b>	COR07a	COR07b	COR07c	COR19	COR02	COR03	COR14	Average	COR15a	COR15b	COR15c	Average	
<b>REE (ppm)</b>													
<b>La</b>	5.3	4.2	4.7	5.3	12.4	7.9	3.4	6.17	30.6	34.4	28.7	31.23	
<b>Ce</b>	10.8	10.9	8.4	11.1	18.2	13.2	5.7	11.19	45.6	67.1	45.3	52.67	
<b>Sm</b>	1.1	0.6	0.7	1.2	1.2	1.2	0.7	0.96	3.9	5.3	4.4	4.53	
<b>Nd</b>	5.6	3.8	3.7	4.9	7.1	5.8	4.1	5	30.4	33.1	25.7	29.73	
<b>Eu</b>	0.1	0.1	0.2	0.2	0.2	0.2	0.2	0.17	1.1	1.7	1.5	1.43	
<b>Pr</b>	1.3	1.2	1	1.3	1.8	1.6	0.9	1.3	7.8	8.9	7.2	7.97	
<b>Gd</b>	0.9	0.7	1	1	0.6	1.5	0.8	0.93	4.4	5.4	4.3	4.7	
<b>Dy</b>	0.6	0.6	0.5	0.8	0.7	1.1	0.9	0.74	3.7	4.1	4.4	4.07	
<b>Er</b>	0.4	0.3	0.3	0.5	0.2	0.6	0.7	0.43	2.1	2.3	2.1	2.17	
<b>Tb</b>	< 0.1	0.1	< 0.1	< 0.1	< 0.1	0.1	0.1	0.1	0.6	0.8	0.7	0.7	
<b>Tm</b>	< 0.1	< 0.1	< 0.1	< 0.1	< 0.1	0.1	0.1	0.1	0.3	0.4	0.4	0.37	
<b>Y</b>	5.2	4.4	4.8	4.3	3.4	5.2	4.1	4.49	19.1	28.5	25.3	24.3	
<b>Yb</b>	0.5	0.3	0.2	0.4	0.3	0.4	0.6	0.39	2.1	2.8	3.4	2.77	
<b>Ratio (ppm)</b>													
<b>(La/Yb)CN</b>	7.6	10.04	16.86	9.5	29.65	14.17	4.06	13.13	10.45	8.81	6.05	8.44	
<b>(La/Sm)CN</b>	3.11	4.52	4.33	2.85	6.67	4.25	3.14	4.12	5.07	4.19	4.21	4.49	
<b>(Gd/Yb)CN</b>	1.49	1.93	4.14	2.07	1.65	3.1	1.1	2.21	1.73	1.6	1.05	1.46	
<b>Eu/Eu*</b>	0.1	0.15	0.24	0.18	0.24	0.15	0.27	0.19	0.27	0.32	0.34	0.31	
<b>ΣREE</b>	31.8	27.2	25.5	31	46.1	38.9	22.3	31.83	152.3	195.7	154.3	167.43	
<b>ΣLREE</b>	25.1	21.5	19.7	25	41.5	31.4	15.8	25.71	123.8	155.9	117.1	132.27	
<b>ΣHREE</b>	6.7	5.7	5.8	6	4.6	7.5	6.5	6.11	28.5	39.8	37.2	35.17	
<b>LREE/HREE</b>	3.75	3.77	3.4	4.17	9.02	4.19	2.43	4.39	4.34	3.92	3.15	3.8	

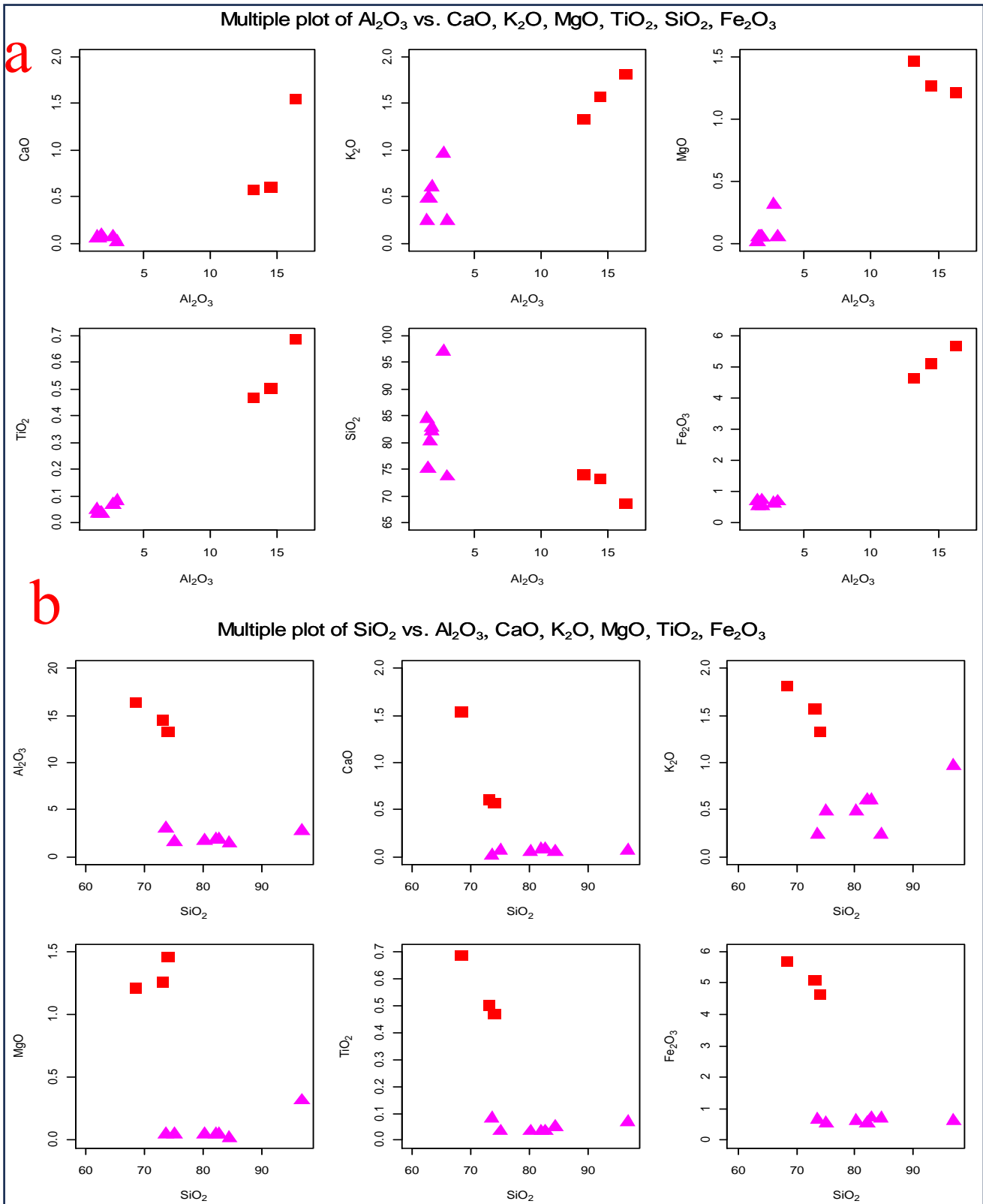


**Fig. 9** Haker diagram variation of metasedimentary rocks in the Taneka Area, (a) Show the relationship between  $Al_2O_3$  with the others major oxides; (b) show the relationship between  $SiO_2$  and the other major oxide.

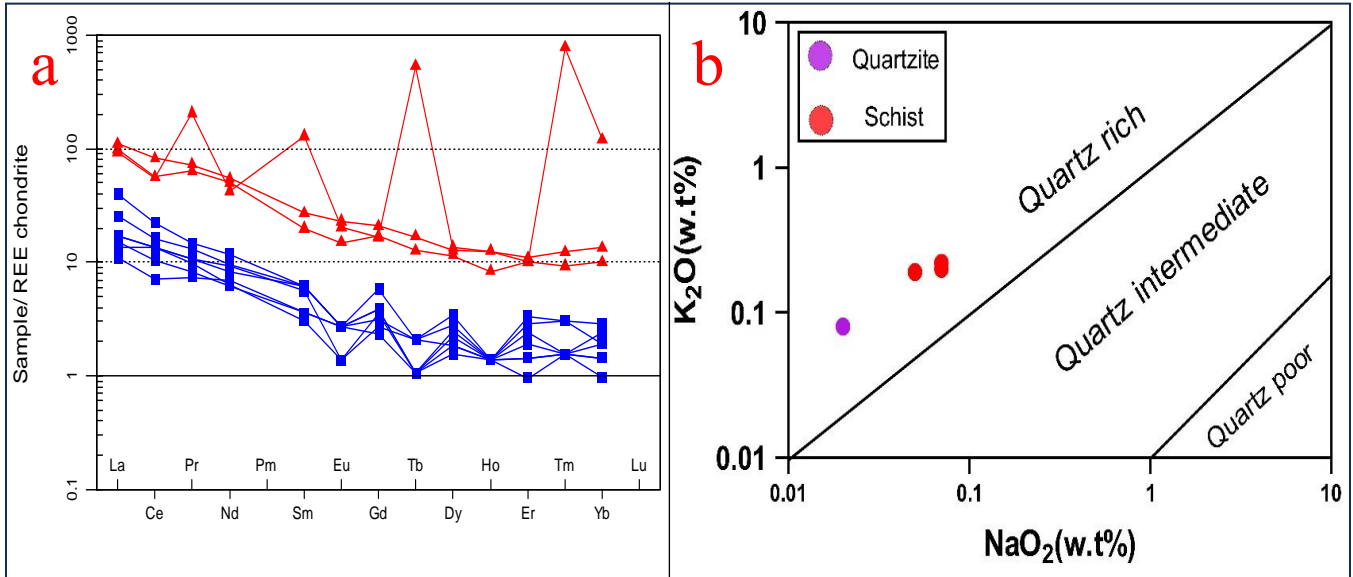


Fig. 10 (a)REE patterns of the metasedimentary rocks in the Tanekas area, red represents the schists, and blue indicates the quartzite samples, and (b)K<sub>2</sub>O (W%) plot against Na<sub>2</sub>O (W.t%) is used to classify the Taneka metasedimentary rocks.

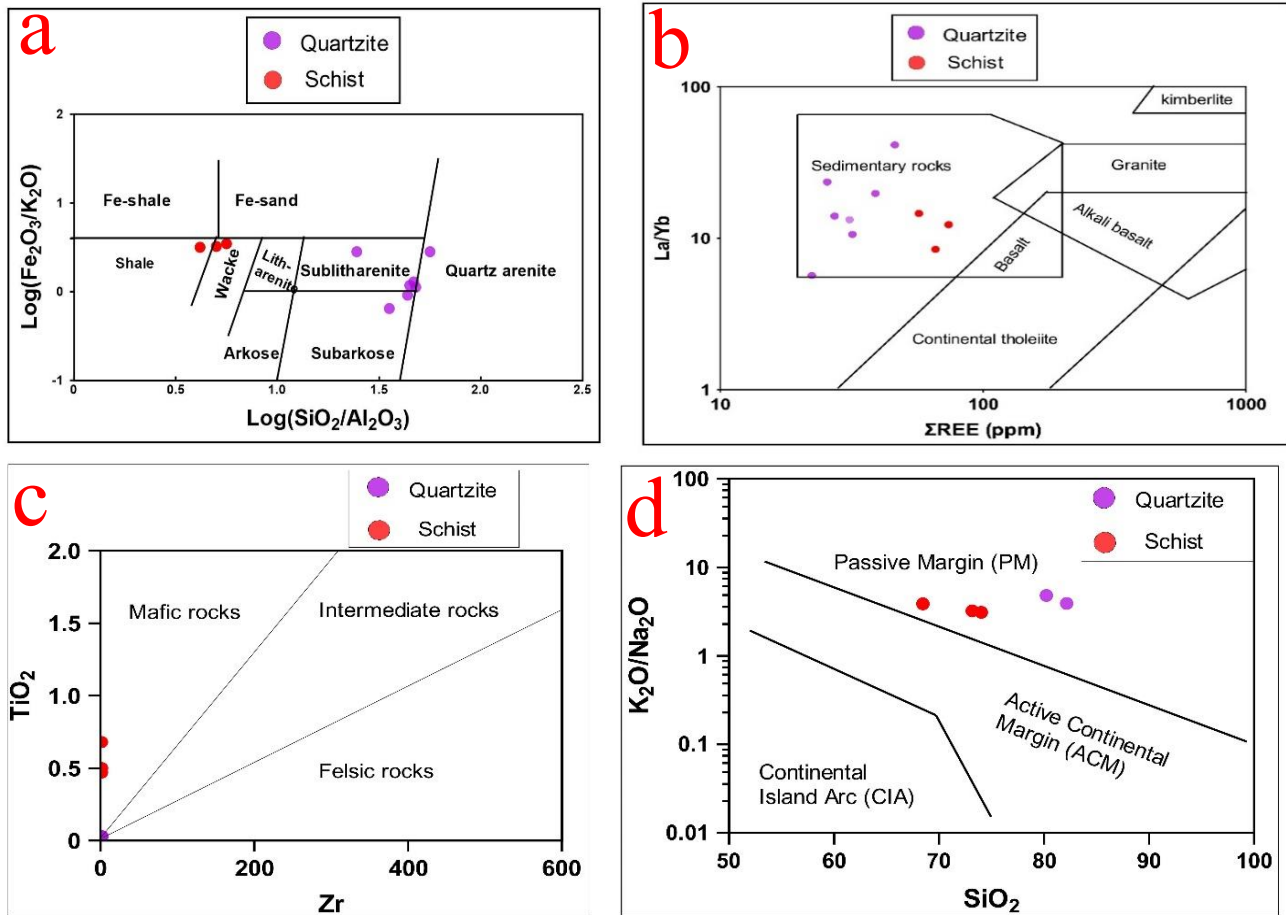


Fig. 11 (a)Discrimination plots  $\log(\text{SiO}_2/\text{Al}_2\text{O}_3)$  against  $\log(\text{Fe}_2\text{O}_3/\text{K}_2\text{O})$  after [47] showing metasedimentary rocks composition, (b)Provenance discrimination plot La/Yb against  $\Sigma\text{REE}$  (c)Discrimination plot  $\text{TiO}_2$  vs Zr plot of quartzite; (d) $\text{K}_2\text{O}/\text{Na}_2\text{O}$  versus  $\text{SiO}_2$  plot of quartzite in the study area, after [48]

## 6. Conclusion

This study elucidates the petrogenesis, tectonic setting, and provenance of the metasedimentary rocks in Taneka Mountain, revealing that the quartzites originated from mature quartz-rich sediments in a passive continental margin, whereas the schists formed from pelitic protoliths in a transitional tectonic environment influenced by nearby active zones. Petrographic analyses confirmed greenschist-facies metamorphism, with quartzites dominated by quartz and muscovite and schists characterized by talc-chlorite assemblages, reflecting distinct sedimentary sources and metamorphic histories. Geochemical signatures further differentiate these lithologies, with quartzites showing felsic affinities and schists exhibiting mixed felsic-mafic contributions, consistent with their deposition along the margin of the Pan-African Dahomeyide orogen. Structural evidence, including recumbent folds and NE-SW fractures, underscores a polyphase deformational history linked to orogenic processes.

These findings enhance our understanding of the evolution of the Taneka Terrane and its role within the broader Dahomeyide belt, highlighting the importance of integrated petrographic and geochemical approaches in reconstructing ancient tectonic environments. Future geochronological and isotopic studies could further constrain the timing of sedimentation and metamorphism, refining regional tectonic models.

## Funding Statement

The African Union Commission funded this research through the Pan African University Life and Earth Sciences Institute (including Health and Agriculture), Ibadan, Nigeria.

## Acknowledgement

This work was conducted as part of the first author's Msc studies. He would like to express his sincere gratitude to Author 2 and 3 for their invaluable guidance, insightful feedback, and continuous support throughout this research.

## References

- [1] Y. Agbossoumondé, R.P. Ménot, and P.M. Nudé, "Geochemistry and Sm-Nd Isotopic Composition of the Agou Igneous Complex (AIC) from the Pan-African Orogen in Southern Togo, West Africa: Geotectonic Implications," *Journal of African Earth Sciences*, vol. 82, pp. 88–99, 2013. [[CrossRef](#)] [[Google Scholar](#)] [[Publisher Link](#)]
- [2] Felix Aidoo et al., "New Insight into the Dahomeyide Belt of Southeastern Ghana, West Africa: Evidence of arc-Continental Collision and Neoproterozoic Crustal Reworking," *Precambrian Research*, vol. 347, 2020. [[CrossRef](#)] [[Google Scholar](#)] [[Publisher Link](#)]
- [3] Kodjopa Attah, and Prosper M. Nudé, *Tectonic Significance of Carbonatite and Ultrahigh-Pressure Rocks in the Pan-African Dahomeyide Suture Zone, Southeastern Ghana*, The Geological Society, vol. 297, 2008. [[CrossRef](#)] [[Google Scholar](#)] [[Publisher Link](#)]
- [4] Daniel Kwayisi, Marlina Elburg, and Jeremie Lehmann, "Preserved Ancient Oceanic Lithosphere within the Buem Structural Unit at the Eastern Margin of the West African Craton," *Lithos*, pp. 410–411, 2022. [[CrossRef](#)] [[Google Scholar](#)] [[Publisher Link](#)]
- [5] Daniel Kwayisi et al., "Cryogenian-Ediacaran Crustal Growth and Evolution of the Active Margin of the Dahomeyide Belt, Ghana," *Geological Magazine*, vol. 160, no. 10, pp. 1914–1931, 2023. [[CrossRef](#)] [[Google Scholar](#)] [[Publisher Link](#)]
- [6] P. Affaton et al., "The Dahomeyide Orogen: Tectonothermal Evolution and Relationships with the Volta Basin," *The West African Orogens and Circum-Atlantic Correlatives*, pp. 107-122, 1991. [[CrossRef](#)] [[Google Scholar](#)] [[Publisher Link](#)]
- [7] P. Appel, A. Moller, and V. Schenk, "High-Pressure Granulite Facies Metamorphism in the Pan-African Belt of Eastern Tanzania: P-T-t Evidence against Granulite Formation by Continent Collision," *Journal of Metamorphic Geology*, vol. 16, no. 4, pp. 491-509, 1998. [[CrossRef](#)] [[Google Scholar](#)] [[Publisher Link](#)]
- [8] Kodjopa Attah et al., "Geochemical Characteristics and U–Pb Zircon LA-ICPMS Ages of Granitoids from the Pan-African Dahomeyide Orogen, West Africa," *Journal of African Earth Sciences*, vol. 79, pp. 1-9, 2013. [[CrossRef](#)] [[Google Scholar](#)] [[Publisher Link](#)]
- [9] Fatchessin Bruno Adjo et al., "Petrographic, Geochemical and Structural Characteristics of Gold-Bearing Metasedimentary Rocks from the Atacora Structural Unit, Northwestern Bénin Republic," *Arabian Journal of Geosciences*, vol. 14, 2021. [[CrossRef](#)] [[Google Scholar](#)] [[Publisher Link](#)]
- [10] Carlos E. Ganade et al., "Tightening-up NE Brazil and NW Africa Connections: New U-Pb/Lu-Hf Zircon Data of a Complete Plate Tectonic Cycle in the Dahomey Belt of the West Gondwana Orogen in Togo and Benin," *Precambrian Research*, vol. 276, pp. 24–42, 2016. [[CrossRef](#)] [[Google Scholar](#)] [[Publisher Link](#)]
- [11] Ronald Trompette, "Proterozoic Neoproterozoic (~600 Ma) Aggregation of Western Gondwana: A Tentative Scenario," *Precambrian Research*, vol. 82, no. 1-2, pp. 101-112, 1997. [[CrossRef](#)] [[Google Scholar](#)] [[Publisher Link](#)]
- [12] Lenka Baratoux, Mark W. Jessell, and Alain N. Kouamelan, "The West African Craton," *The Geology of North Africa*, Springer, Cham, pp. 47–68, 2023. [[CrossRef](#)] [[Google Scholar](#)] [[Publisher Link](#)]
- [13] Nasser Ennih, and Jean-Paul Liégeois, *The Boundaries of the West African Craton, with Special Reference to the Basement of the Moroccan Metacratonic Anti-Atlas Belt*, Geological Society Special Publication, 2008. [[CrossRef](#)] [[Google Scholar](#)] [[Publisher Link](#)]
- [14] Nasser Ennih, and Jean-Paul Liégeois, "The Moroccan Anti-Atlas: The West African Craton Passive Margin with Limited Pan-African Activity. Implications for the Northern Limit of the Craton," *Precambrian Research*, vol. 112, no. 3-4, pp. 289-302, 2001. [[CrossRef](#)] [[Google Scholar](#)] [[Publisher Link](#)]

- [15] R. Black et al., “Pan-African Displaced Terranes in the Tuareg Shield (Central Sahara),” *Geology*, vol. 22, no. 7, pp. 641-644, 1994. [[CrossRef](#)] [[Google Scholar](#)] [[Publisher Link](#)]
- [16] Kodjopa Attoh, R.D. Dallmeyer, and Pascal Affaton, “Chronology of Nappe Assembly in the Pan-African Dahomeyides Orogen, West Africa: Evidence from  $^{40}\text{Ar}^{39}\text{Ar}$  Minerals Age,” *Precambrian Research*, vol. 82, no. 1-2, pp. 153-171, 1997. [[CrossRef](#)] [[Google Scholar](#)] [[Publisher Link](#)]
- [17] Jean Paul Liégeois et al., “The LATEA Meta-Craton (Central Hoggar, Tuareg Shield, Algeria): Behavior of an Old Passive Margin During the Pan-African Orogeny,” *Journal of African Earth Sciences*, vol. 37, no. 3-4, pp. 161-190, 2003. [[CrossRef](#)] [[Google Scholar](#)] [[Publisher Link](#)]
- [18] Luc Adissin Glodji, “*The Kandi Shear Zone and Associated Magmatism in the Savalou-Dassa Region (Benin): Structural, Petrological and Geochronological Study*,” Hall Theses, pp. 1-277, 2012. [[Google Scholar](#)] [[Publisher Link](#)]
- [19] Daniel Kwayisi, Jeremie Lehmann, and Marlina Elburg, “Provenance and Depositional Setting of the Buem Structural Unit (Ghana): Implications for the Paleogeographic Reconstruction of the West African and Amazonian Cratons in Rodinia,” *Gondwana Research*, vol. 109, pp. 183–204, 2022. [[CrossRef](#)] [[Google Scholar](#)] [[Publisher Link](#)]
- [20] Y. Agbossoumonde, and R.P. Menot, “Geochemical Characterization of High-Pressure Basic Granulites from the Agou Massif in the Pan-African Dahomeyide Chain in Southern Togo,” *Journal of Scientific Research of the University of Lomé*, vol. 7, no. 2, 2005. [[CrossRef](#)] [[Google Scholar](#)] [[Publisher Link](#)]
- [21] Pascal Affaton, Jean Sougy, and Roland Trompette, “The Tectono-stratigraphic Relationship between The Upper Precambrian and Lower Paleozoic Volta Basin and The Pan-African Dahomeyides Orogenic Belt (West Africa),” *American Journal of Science*, vol. 280, no. 3, pp. 224–248, 1980. [[CrossRef](#)] [[Google Scholar](#)] [[Publisher Link](#)]
- [22] Norbert Clauer et al., “Geochronology of Sedimentary and Metasedimentary Precambrian Rocks of the West African Craton,” *Precambrian Research*, vol. 18, no. 1-2, pp. 53-71, 1982. [[CrossRef](#)] [[Google Scholar](#)] [[Publisher Link](#)]
- [23] L. Cahen et al., *The Geochronology and Evolution of Africa*, Clarendon Press, Oxford, England, pp. 181-183, 1984. [[Google Scholar](#)]
- [24] sPascal Affaton, “*The Volta Basin (West Africa) a Passive Margin, of Late Proterozoic Age, Tectonized in the Pan-African (600 ± 50 Ma)*,” Doctoral Thesis, Université Aix-Marseilles III, 1987. [[Google Scholar](#)] [[Publisher Link](#)]
- [25] Pascal Affaton, Luis Aguirre, and Rene-Pierre Ménot, “Thermal and Geodynamic Setting of the Buem Volcanic Rocks Near Tiélé, Northwest Bénin, West Africa,” *Precambrian Research*, vol. 82, no. 3-4, pp. 191-209, 1997. [[CrossRef](#)] [[Google Scholar](#)] [[Publisher Link](#)]
- [26] Shiloh Osae et al., “Provenance and Tectonic Setting of the Late Proterozoic Buem Sandstones of Southeastern Ghana: Evidence from Geochemistry and Detrital Modes,” *Journal of African Earth Sciences*, vol. 44, no. 1, pp. 85-96, 2006. [[CrossRef](#)] [[Google Scholar](#)] [[Publisher Link](#)]
- [27] Daniel Kwayisi et al., “Two Suites of Gabbros in the Buem Structural Unit, of the Pan-African Dahomeyides Orogen, Southeastern Ghana: Constraints from the New Field and Geochemical Data,” *Journal of African Earth Sciences*, vol. 129, pp. 45-55, 2017. [[CrossRef](#)] [[Google Scholar](#)] [[Publisher Link](#)]
- [28] Luc Adissin Glodji et al., “Geology and Geochemistry of the Chromiferous Mineralization in the External Zone of the Pan-African Dahomeyides Belt, Northwestern Benin (Gulf of Guinea, West Africa),” *International Journal of Geosciences*, vol. 10, no. 12, pp. 1068-1080, 2019. [[CrossRef](#)] [[Google Scholar](#)] [[Publisher Link](#)]
- [29] Fatchessin Bruno Adjo et al., “A Review of the Current State of Knowledge on Gold Mineralization in Benin Republic, West Africa,” *Applied Earth Science*, vol. 128, no. 1, pp. 2-14, 2019. [[CrossRef](#)] [[Google Scholar](#)] [[Publisher Link](#)]
- [30] Fatchessin Bruno Adjo et al., “Geochemistry of Gold-Bearing Metamorphic Rocks of the Natitingou Area, Atacora Structural Unit, Northwestern Bénin (West Africa): Implications for Au Genesis,” *Geochemistry*, vol. 81, no. 2, 2021. [[CrossRef](#)] [[Google Scholar](#)] [[Publisher Link](#)]
- [31] R.P. Menot, “The Basic and Ultrabasic Massifs of the Pan-African Mobile Zone in Ghana, Togo and Benin; State of the Question,” *Bulletin of the Geological Society of France*, vol. 3, pp. 297-303, 1980. [[CrossRef](#)] [[Google Scholar](#)] [[Publisher Link](#)]
- [32] Kodjopa Attoh, and Jennifer Morgan, “Geochemistry of High-Pressure Granulites from the Pan-African Dahomeyide Orogen, West Africa: Constraints on the Origin and Composition of the Lower Crust,” *Journal of African Earth Sciences*, vol. 39, no. 3-5, pp. 201–208, 2004. [[CrossRef](#)] [[Google Scholar](#)] [[Publisher Link](#)]
- [33] Y. Agbossoumondé et al., “Petrological and Geochronological Constraints on the Origin of the Palimé- Amlamé Granitoids (South Togo, West Africa): A Segment of the West African Craton Paleoproterozoic Margin Reactivated During the Pan-African Collision,” *Gondwana Research*, vol. 12, no. 4, pp. 476-488, 2007. [[CrossRef](#)] [[Google Scholar](#)] [[Publisher Link](#)]
- [34] Prosper M. Nude et al., “Petrography and Chemical Evidence for Multi-stage Emplacement of Western Buem Volcanic Rocks in the Dahomeyide Orogenic Belt, Southeastern Ghana, West Africa,” *Journal of African Earth Sciences*, vol. 112, pp. 314-327, 2015. [[CrossRef](#)] [[Google Scholar](#)] [[Publisher Link](#)]
- [35] Daniel Kwayisi, Jeremie Lehmann, and Marlina Elburg, “The Architecture of the Buem Structural Unit: Implications for the Tectonic Evolution of the Pan-African Dahomeyide Orogen, West Africa,” *Precambrian Research*, vol. 338, 2020. [[CrossRef](#)] [[Google Scholar](#)] [[Publisher Link](#)]

- [36] Stephane Guillot et al., “Transition from Subduction to Collision Recorded in the Pan-African arc Complexes (Mali to Ghana),” *Precambrian Research*, vol. 320, pp. 261-280, 2019. [[CrossRef](#)] [[Google Scholar](#)] [[Publisher Link](#)]
- [37] Renaud Caby, “Precambrian Terranes of Benin, Nigeria, and Northeast Brazil and the Late Proterozoic South Atlantic Fit,” *Geological Society of America Special Paper*, 1989. [[CrossRef](#)] [[Google Scholar](#)] [[Publisher Link](#)]
- [38] D. Chala et al., “Pan-African Deformation Markers in the Migmatitic Complexes of Parakou-Nikki (Northeast Benin),” *Journal of African Earth Sciences*, vol. 111, pp. 387-398, 2015. [[CrossRef](#)] [[Google Scholar](#)] [[Publisher Link](#)]
- [39] Feiko Kalsbeek, Dirk Frei, and Pascal Affaton, “Constraints on Provenance, Stratigraphic Correlation and Structural Context of the Volta Basin, Ghana, from Detrital Zircon Geochronology: An Amazonian Connection?,” *Sedimentary Geology*, vol. 212, no. 1-4, pp. 86–95, 2008. [[CrossRef](#)] [[Google Scholar](#)] [[Publisher Link](#)]
- [40] L. Adissin Glodji et al., “Geochronology and Geochemistry of Igneous Rocks of the Dassa Region, Central-Benin: Evidence of an Ediacaran Emplacement of Alkali-Calcic and Alkaline Plutonic and Volcanic Magmas,” *International Journal of Earth Sciences*, vol. 112, pp. 1331-1360, 2023. [[CrossRef](#)] [[Google Scholar](#)] [[Publisher Link](#)]
- [41] Renaud Caby, “Terrane Assembly and Geodynamic Evolution of Central-Western Hoggar: A Synthesis,” *Journal of African Earth Sciences*, vol. 37, no. 3–4, pp. 133–159, 2003. [[CrossRef](#)] [[Google Scholar](#)] [[Publisher Link](#)]
- [42] R. Caby, and J.M. Boesse, “Pan-African Nappe System in Southwest Nigeria: The Ife-Ilesha Schist Belt,” *Journal of African Earth Sciences*, vol. 33, no. 2, pp. 211-225, 2001. [[CrossRef](#)] [[Google Scholar](#)] [[Publisher Link](#)]
- [43] Mahaman Sani Tairou et al., “Pan-African Paleostresses and Reactivation of the Eburnean Basement Complex in Southeast Ghana (West Africa),” *Journal of Geological Research*, vol. 2012, no. 1, pp. 1-15, 2012. [[CrossRef](#)] [[Google Scholar](#)] [[Publisher Link](#)]
- [44] C.Y. Anani et al., “Provenance of Sandstones from the Neoproterozoic Bombouaka Group of the Volta Basin, Northeastern Ghana,” *Arabian Journal of Geosciences*, vol. 10, 2017. [[CrossRef](#)] [[Google Scholar](#)] [[Publisher Link](#)]
- [45] B.W.D. Yardley, “Turner Metamorphic Petrology: Mineralogical, Field and Tectonic Aspects. 2nd Edition. Washington, New York, and London (McGraw Hill), 1981. xv+ 524 pp., 162 figs. Price £26.95,” *Mineralogical Magazine*, vol. 46, no. 339, pp. 278–279, 1982. [[CrossRef](#)] [[Google Scholar](#)] [[Publisher Link](#)]
- [46] Helmut G.F. Winkler, *Petrogenesis of Metamorphic Rocks*, 5<sup>th</sup> ed., Springer New York, NY, 1979. [[CrossRef](#)] [[Google Scholar](#)] [[Publisher Link](#)]
- [47] Michael M. Herron, “Geochemical Classification of Terrigenous Sands and Shales from Core or Log Data,” *Journal of Sedimentary Petrology*, vol. 58, no. 5, pp. 820–829, 1988. [[CrossRef](#)] [[Google Scholar](#)] [[Publisher Link](#)]
- [48] B.P. Roser, and R.J. Korsch, “Determination of Tectonic Setting of Sandstone-Mudstone Suites Using SiO<sub>2</sub> Content and K<sub>2</sub>O/Na<sub>2</sub>O Ratio,” *The Journal of Geology*, vol. 94, no. 5, 1986. [[CrossRef](#)] [[Google Scholar](#)] [[Publisher Link](#)]
- [49] Mukul R. Bhatia, “Plate Tectonics and Geochemical Composition of Sandstones,” *The Journal of Geology*, vol. 91, no. 6, 1983. [[CrossRef](#)] [[Google Scholar](#)] [[Publisher Link](#)]
- [50] S.M. McLennan, “Rare Earth Elements in Sedimentary Rocks: Influence of Provenance and Sedimentary Processes,” *Reviews in Mineralogy and Geochemistry*, pp. 169–200, 2018. [[CrossRef](#)] [[Google Scholar](#)] [[Publisher Link](#)]
- [51] Stuart Ross Taylor, and Scott M. McLennan, *The Continental Crust: Its Composition and Evolution*, Blackwell Scientific Publications, pp. 1-312, 1985. [[Google Scholar](#)] [[Publisher Link](#)]
- [52] Olusegun G. Olisa, Olugbenga A. Okunlola, and Ayotunde A. Omitogun, “Petrochemistry and Petrogenetic Features of Metasedimentary Rocks of Igangan Area, Southwestern Nigeria,” *Journal of Geoscience and Environment Protection*, vol. 6, no. 4, 2018. [[CrossRef](#)] [[Google Scholar](#)] [[Publisher Link](#)]
- [53] Young Ezenwa Obioha, “Geochemistry Evolution of Schists of Northwest Obudu Area Southeastern Nigeria,” *Global Journal of Geological Sciences*, vol. 19, no. 1, 2021. [[CrossRef](#)] [[Google Scholar](#)] [[Publisher Link](#)]
- [54] H. Wani, “REE Characteristics and REE Mixing Modeling of the Proterozoic Quartzites and Sandstones,” *International Journal of Geosciences*, vol. 8, no. 1, pp. 16-29, 2017. [[CrossRef](#)] [[Google Scholar](#)] [[Publisher Link](#)]
- [55] Barth N. Ekwueme, and Bassey E. Ephraim, “Rare Earth Element Geochemistry and Protoliths of Schists in Southeast Lokoja, Central Nigeria,” *Global Journal of Geological Sciences*, vol. 3, no. 1, pp. 9-15, 2005. [[CrossRef](#)] [[Google Scholar](#)] [[Publisher Link](#)]
- [56] M.S. Kolawole, E.C. Chukwu, and A.N. Agibe, “Geochemistry and Petrogenetic Evolution of Metasedimentary Rocks in Bunu Area, Part of Kabba-Lokoja-Igarra Schist Belt, SW Nigeria,” *Acta Geochimica*, vol. 41, pp. 765–788, 2022. [[CrossRef](#)] [[Google Scholar](#)] [[Publisher Link](#)]
- [57] Luiza de Carvalho Mendes, Ticiano Jose Saraiva Dos Santos, and Nadia Borges Gomes, “Geochemistry and Provenance of the Metasedimentary Rocks Surrounding the Santa Quitéria Magmatic Arc, NE Brazil: Tectonic and Paleogeographic Implications for the Assembly of West Gondwana,” *Precambrian Research*, vol. 356, 2021. [[CrossRef](#)] [[Google Scholar](#)] [[Publisher Link](#)]
- [58] R.A. Obasi, and H.Y. Madukwe, “Use of Geochemistry to Study the Provenance, Tectonic Setting, Source-Area Weathering and Maturity of Igarra Marble, Southwest, Nigeria,” *American Journal of Engineering Research*, vol. 5, no. 6, pp. 90–99, 2016. [[Google Scholar](#)] [[Publisher Link](#)]

- [59] Parampreet Kaur et al., “Geochemical Constraints on the Provenance and Tectonic Setting of Metasedimentary Rocks from the South Delhi Supergroup, NW India: Implications for Tectonic Evolution of the Western Margin of the Aravalli Orogen,” *International Geology Review*, vol. 66, no. 6, pp. 1280-1301, 2024. [[CrossRef](#)] [[Google Scholar](#)] [[Publisher Link](#)]
- [60] Sory I.M. Konate et al., “Provenance and Tectonic Setting of Greywacke and Siltstone of the Nampala Gold Deposit, Southern Mali,” *Applied Earth Science: Transactions of the Institutions of Mining and Metallurgy*, vol. 133, no. 2, pp. 129-147, 2024. [[CrossRef](#)] [[Google Scholar](#)] [[Publisher Link](#)]
- [61] Blestmond A. Brako et al., “Petrography and Geochemistry of Metasedimentary Rocks from the Paleoproterozoic Birimian at the Chagupana Area, North-west Ghana: Implications for Provenance and Tectonic Setting,” *Arabian Journal of Geosciences*, vol. 15, 2022. [[CrossRef](#)] [[Google Scholar](#)] [[Publisher Link](#)]
- [62] Theophilus Kekeli Agbenyezi et al., “Paleoweathering, Provenance and Tectonic Setting of Metasedimentary Rocks at the Ayanfuri Area in the Paleoproterozoic Kumasi Basin in Ghana: Evidence from Petrography and Geochemistry,” *Journal of Sedimentary Environments*, vol. 7, pp. 519-538, 2022. [[CrossRef](#)] [[Google Scholar](#)] [[Publisher Link](#)]
- [63] Ajay K. Singh et al., “Age, Provenance and Tectonic Setting of Metasedimentary Rocks of the Simlipal Complex, Singhbhum Craton, Eastern India,” *Precambrian Research*, vol. 355, 2021. [[CrossRef](#)] [[Google Scholar](#)] [[Publisher Link](#)]